



Contents lists available at ScienceDirect

Journal of Biomechanics

journal homepage: www.elsevier.com/locate/jbiomech
www.JBiomech.com

A novel approach to predicting human ingress motion using an artificial neural network

Younguk Kim, Eun Soo Choi, Jungmi Seo, Woo-sung Choi, Jeonghwan Lee, Kunwoo Lee *

Department of Mechanical and Aerospace Engineering, Seoul National University, Seoul, Republic of Korea

ARTICLE INFO

Article history:

Accepted 5 December 2018

Keywords:

Human motion simulation
Neural network-based motion prediction
Human motion database
Vehicle ingress motion
Digital human modeling

ABSTRACT

Due to the increased availability of digital human models, the need for knowing human movement is important in product design process. If the human motion is derived rapidly as design parameters change, a developer could determine the optimal parameters. For example, the optimal design of the door panel of an automobile can be obtained for a human operator to conduct the easiest ingress and egress motion. However, acquiring motion data from existing methods provides only unrealistic motion or requires a great amount of time. This not only leads to an increased time consumption for a product development, but also causes inefficiency of the overall design process. To solve such problems, this research proposes an algorithm to rapidly and accurately predict full-body human motion using an artificial neural network (ANN) and a motion database, as the design parameters are varied. To achieve this goal, this study refers to the processes behind human motor learning procedures. According to the previous research, human generate new motion based on past motion experience when they encounter new environments. Based on this principle, we constructed a motion capture database. To construct the database, motion capture experiments were performed in various environments using an optical motion capture system. To generate full-body human motion using this data, a generalized regression neural network (GRNN) was used. The proposed algorithm not only guarantees rapid and accurate results but also overcomes the ambiguity of the human motion objective function, which has been pointed out as a limitation of optimization-based research. Statistical criteria were utilized to confirm the similarity between the generated motion and actual human motion. Our research provides the basis for a rapid motion prediction algorithm that can include a variety of environmental variables. This research contributes to an increase in the usability of digital human models, and it can be applied to various research fields.

© 2018 Elsevier Ltd. All rights reserved.

1. Introduction

Digital human models are being increasingly used in a variety of industries, including ergonomics, virtual surgery, product design, and vehicle design (Jung et al., 2009; Lee et al., 2009; Rasmussen et al., 2003). The benefit of using a digital model for musculoskeletal simulation is that it enables the study of if-then scenarios in many research areas, as non-invasive evaluation of muscles and joints is made possible (Gerus et al., 2013; Marra et al., 2015; Fregly, 2009). Most of these researches are based on the premise that human motion is known data through motion capture or other methods. For example, Masoud et al. (2016) proposed a mathemat-

ical model of the relation between human ingress motion and discomfort using motion captured data (Masoud et al., 2016). However, human motion acquired from experiments is difficult to apply to various environments, because only discontinuous motion for limited input variables can be provided. Therefore, the development of motion prediction algorithms for various input environmental variables enhances the usability of digital human models.

The fields of recording, tracking, and predicting human motion in various environments have been studied extensively. Two typical methods are the motion capture-based approach and the optimization-based approach (Chaffin, 2002; Moeslund et al., 2006). The first method captures actual human motion through an optical/inertial motion capture device and reproduces the results virtually. This approach has a high degree of accuracy, and it has been applied to product research and design (Kim and Lee, 2009; Kim et al., 2012). However, it can only provide discon-

* Corresponding author at: Department of Mechanical and Aerospace Engineering, Seoul National University, 1 Gwanak-ro, Daehak-dong, Gwanak-gu, Seoul 151-744, Republic of Korea.

E-mail address: kunwoohcl@gmail.com (K. Lee).

tinuous human motion output data for limited input variables, which makes it difficult to predict motion for situations in which experiments have not been previously conducted.

To overcome this problem, the optimization-based motion prediction algorithm using a human action strategy as an objective function was developed. Rasmussen et al. (2000) demonstrated this method with a simple pedaling model without verification. They called this approach “inverse-inverse dynamics,” because it constructed an inner loop that has inverse dynamics and an outer loop that optimizes the control points of the human motion curve with a user-defined objective function (Rasmussen et al., 2000). Abdel-Malek and Arora (2013) summarized such optimization-based human posture and motion prediction algorithms as “predictive dynamics.” Farahani et al. (2016) conducted a study to predict and verify closed-chain human arm movement with velocity-dependent viscous force.

Since most of these studies have found solutions through optimization, a local minimum issue is inevitable. In finding a solution through optimization, the inability to guarantee the global optimum raises uncertainty about the robustness of the solution. In addition, these approaches take 1–40 min to generate a single action, resulting in delayed task completion (Bataineh et al., 2016). Moreover, to formulate optimization-based motion prediction, it is necessary to define a valid objective function. Many studies have proposed various objective functions, such as joint torque (Xiang et al., 2009) and metabolic cost (Farahani et al., 2016), but the objective function of these studies was limited to a specific task and could not be adapted to general motion. This challenge means that it is difficult to find a well-defined objective function to predict human motion generally, and the resulting ambiguity makes it difficult to apply optimization to real product design.

Through formulations of the relationship between the external environment and parametric human motion, our research predicts human motion that is not actually measured. For this purpose, we were motivated by the human motor learning procedure. Human cognitive systems generate motion in new environments by drawing on similar past experience (Aggarwal and Cai, 1999; Wagner and Smith 2008; Dretsches and Tipples, 2008; Kumar et al., 2014). The proposed algorithm uses a motion database for “past experience” and ANN for “recall of past experience.” ANNs are mathematical models that predict the output of systems, inspired by the structure and function of human biological neural networks. They are widely used in digital human modeling problems due to their ability to solve high-level problems and achieve successful results (Bataineh et al., 2016; Bu et al., 2009; Oh et al., 2013; Zhang et al., 2010).

Due to the complexity of human motion and the difficulty of building a motion database, ANNs have only been applied to specific scenarios in digital human model problems. Past research has only investigated human posture prediction and motion generated by the results of predictive dynamics (Bataineh et al., 2013, 2016; Zhang et al., 2010). To overcome this point, we conducted motion capture experiments of actual human motion in various parameterized environments. We constructed a human motion network that corresponds to the input environment with captured motion database. We used a radial-basis network (RBN) rather than the widely used feed-forward backpropagation network, because a feed-forward backpropagation network is not as efficient as an RBN when a large number of output problems must be simulated with a limited number of databases. This type of network characteristic is adaptable to human motion prediction research (Bataineh, 2015), and it provides a global solution to optimize the network parameters.

This research focuses on the prediction of vehicle ingress motion by utilizing a proposed algorithm. A volume of research related to vehicle design has been conducted to analyze ingress

motion. Kim & Lee formulated a relationship between force exerted by the muscles and ingress discomforts in ingress motion by using fuzzy logic (Kim and Lee, 2009). Masoud analyzed ingress motion using support vector machine and UMPCA to analyze the importance of joint (Masoud et al., 2016; Masoud et al., 2017). Most research works, including previously mentioned ones, assume that ingress motion is based on known data through experiment. Due to the assumptions based on experimental data, such works not only require high costs to conduct experiments, but also are limited by a few selected variables. In this research, an algorithm is proposed to predict ingress motion rapidly and accurately, and is expected to overcome such limitations.

In this study, motion prediction based on ANN is used to predict motion for a full-body human model with 31 degrees of freedom (DOF). This allows the prediction of various motions, including those not conducted in experiments. In addition, our research guarantees a faster speed than previous optimization approaches while also eliminating the ambiguity of objective functions. Finally, based on an actual human motion capture database, we improve the accuracy of prediction compared with existing research. The following sections present the details of our approach.

2. Method

2.1. Experimental study

2.1.1. Subject information

Ten healthy subjects (age 25.5 ± 5 years, height 1.8 ± 0.05 m) volunteered for this study. All the subjects were reported to be free of injury before and during the trial. We collected information about people without muscle, ligament, or joint disease. Before the experiment, our research team provided test procedures, protocols, and potential risk for participating to the subjects. Written informed consent from the participant subject was obtained. The experiment was approved by the Ethics Committee of Seoul National University (IRB).

2.1.2. Experiment instrument

For motion capture, reflective infrared markers were attached to the subjects, according to the plug in gait marker set (Davis et al., 1991). For a system to catch the behavior of the feet with enhanced accuracy, additional markers were attached to three locations: medial most protrusion of the first metatarsal head, lateral most protrusion of the fifth metatarsal head, and medial malleolus in each foot segment. The specific locations are shown in Fig. 1(c). The three-dimensional position of each marker was measured with a motion capture system (12 cameras, MX-T160, Vicon, Oxford, UK). All cameras were arranged to capture full body motion and the data were sampled at 100 Hz. The force plates are placed at two different locations: one at the front carpet position of the vehicle and the other on the outside of the experimental mock-up. The placement of force plates is described in Fig. 1(a). The subjects performed a vehicle ingress motion in various environments. For this purpose, equipment that reproduces the conditions of a vehicle ingress was constructed with adjustable parts. The equipment used in the experiment and the environmental variables are as shown in Fig. 1. The ingress motion of the subjects was captured in varied vehicle environments. To change the vehicle environments, the four variables (Horizontal Seat Location, Side Width, Door Open Angle, Door trim Extrusion) are adjusted.

2.1.3. Experimental protocol

This experiment measured the motion capture data of the marker and the ground reaction force data. The subjects performed an ingress motion in a given vehicle condition. Fig. 1 describes the

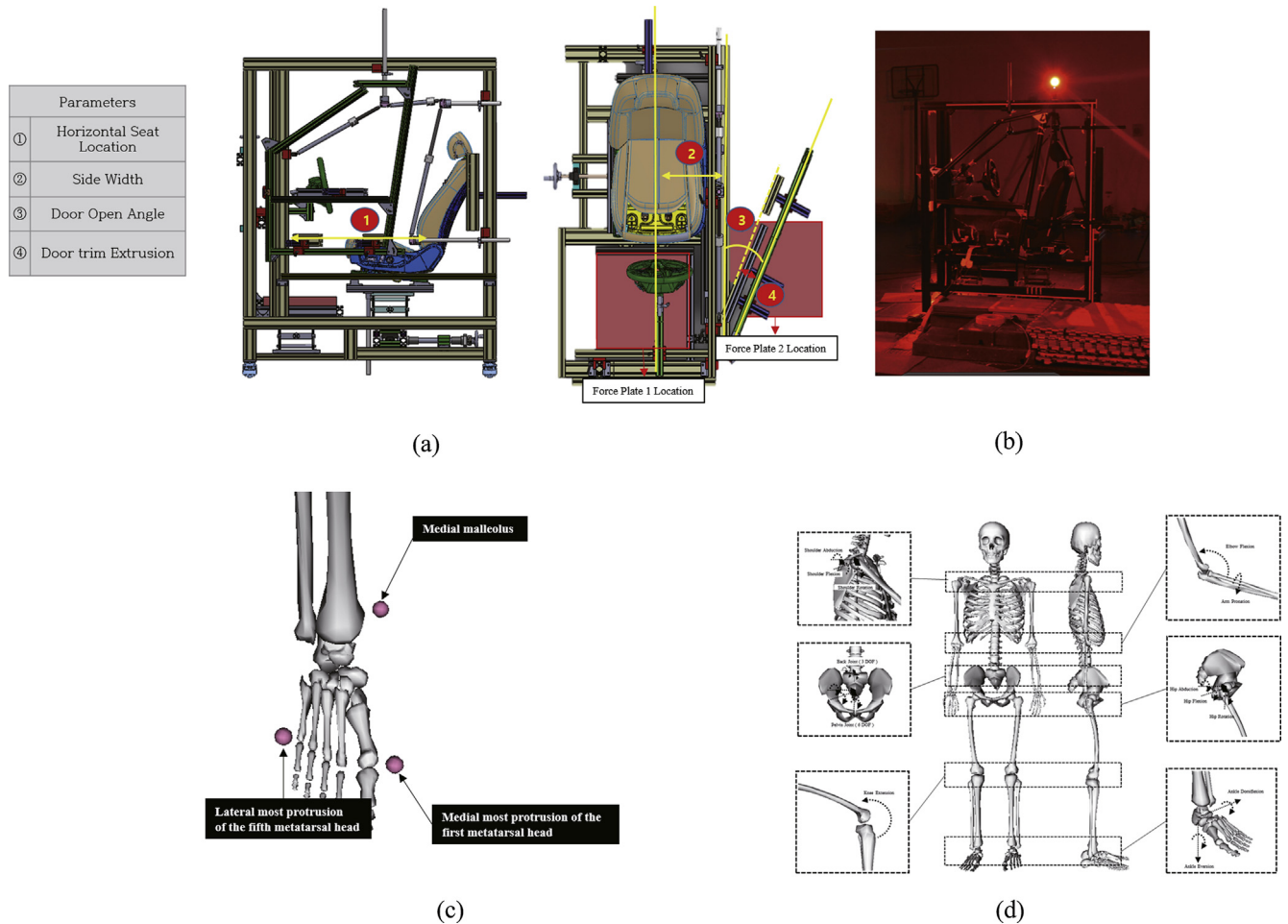


Fig. 1. Parameter of the environment. (a) List of parameter. (b) Actual photo of the environment. (c) Additional marker information. (d) Schematic of the skeleton model for research.

external environment parameters adjusted in the experiment. The experiment was designed based on a central composite design method and was conducted under the following conditions. As each subject steps on the force plate located outside the mock-up, the ingress motion begins to be recorded. After each subject is fully seated in the mock-up, the subject sends an end signal of the motion to the operator. The experiment was performed after a warm-up so that the subject was fully familiar with the experimental environment. To minimize the effect of fatigue, the subjects were instructed to rest between sets.

2.2. Computational study

2.2.1. Data post-processing and inverse kinematics

All marker data captured using the Vicon Nexus motion capture system were labeled manually. For each subject, a subject-specific model of the skeletal model was constructed by using the static marker data and conducting scaling process in OpenSim 3.3 (Delp et al., 2007). In this research, Hamner's Full-body Model was used (Hamner et al., 2010). A description of how the human model in this research was used is shown in Fig. 1(d). The motion capture data extracted through Mokka (Biomechanical ToolKit, Lausanne, Switzerland) was processed into data usable for OpenSim 3.3. All the kinematic and ground reaction force data were resampled at 100 Hz. The marker data were converted to joint angle data through inverse kinematics in OpenSim 3.3. All the individual output data were normalized for the start and end times.

2.2.2. ANN for human body motion

The prediction performance of an ANN is influenced by the input selection, which affects the output value. Therefore, input selection is important for a high classification and an accurate prediction rate in ANN construction (Fernando et al., 2009). In particular, in the case of a human body model, there are a number of input variables determined by individual characteristics. However, the efficiency and accuracy of prediction would worsen if all of these variables are used for learning. Hence, for this study, the dominant variable is selected based on prior research. According to Kim and Lee (2009), the lower limb length is the principal variable in human ingress motion. This research added weight and torso length as input variables to reflect each human anthropometric characteristic. Thus, based on the previous research, height, weight, torso length, and lower limb principal lengths (femur, tibia, and foot) are selected as the input variables. In the case of vehicle variables, four environmental variables were used as input variables, and the number of input dimensions was 10. Prior to learning, all the input variables were normalized by a unit variance. The output variable was the parameterized joint angle curve of each human body. For parameterization, 11 uniform control points were used in each joint angle curve. This research used a cubic spline method to parameterize a joint angle curve. The total number of output dimensions was 341 which is the product of the joint angles and number of control points.

The training input and output in our research had high-dimensional input and output. In a previous study, a vehicle

ingress motion was analyzed by using principal component analysis (Masoud et al., 2017). However, the analysis on targeted vehicle ingress motion resulted in only low classification rate because of the acyclic nature and complexity of the motion. As shown in Fig. 2(a), the linear method could not guarantee accurate results in a high-dimensional, nonlinear problem. Therefore, it was necessary to use a more appropriate algorithm for more accurate “recall of past experience.” To solve this problem, we utilized a generalized regression neural network (GRNN), a type of ANN used to predict nonlinear space. The GRNN used in this research was based on the non-parametric regression of neural networks with radial basis neurons. A mathematical representation of the network is shown below (Eqs. (1) and (2)).

$$\hat{Y}(X) = \frac{\sum_{i=1}^n Y_i \exp\left(-\frac{D_i^2}{2\sigma}\right)}{\sum_{i=1}^n \exp\left(-\frac{D_i^2}{2\sigma}\right)} \quad (1)$$

$$D_i^2 = (x - x_i)^T (x - x_i) \quad (2)$$

where $\hat{Y}(X)$ is the prediction value of the input x and D_i^2 is the square of the distance between the training sample x_i and input x .

The constructed network consists of an input/output layer, radial basis layer, and special linear layer. A block diagram for this design is shown in Fig. 2(b) (Specht, 1991). The training data have 485 pairs of environment and human motion. The input data of training are represented in a 10×485 matrix. The data includes 4 vehicle environment variables and 6 human variables. The output data for training consist of a 341×485 matrix form. The time history of each joint angle motion is parameterized by the cubic spline method, represented by 11 control points. Since each motion is realized by 31 joints, each motion is defined by 341 (11×31) numbers. We used 485 motions for training, thus the data used for training is 341×485 , in total. Detailed information of input and output is shown in Fig. 2(c) and (d). These information constructs GRNN for human motion prediction.

3. Results

Training and execution was conducted on a Windows 10 computer with an Intel Core i7 3.4 GHz processor and 64 GB of RAM. After the training process is completed, this study estimates the time of motion generation. The elapse time was 0.0158 s for the

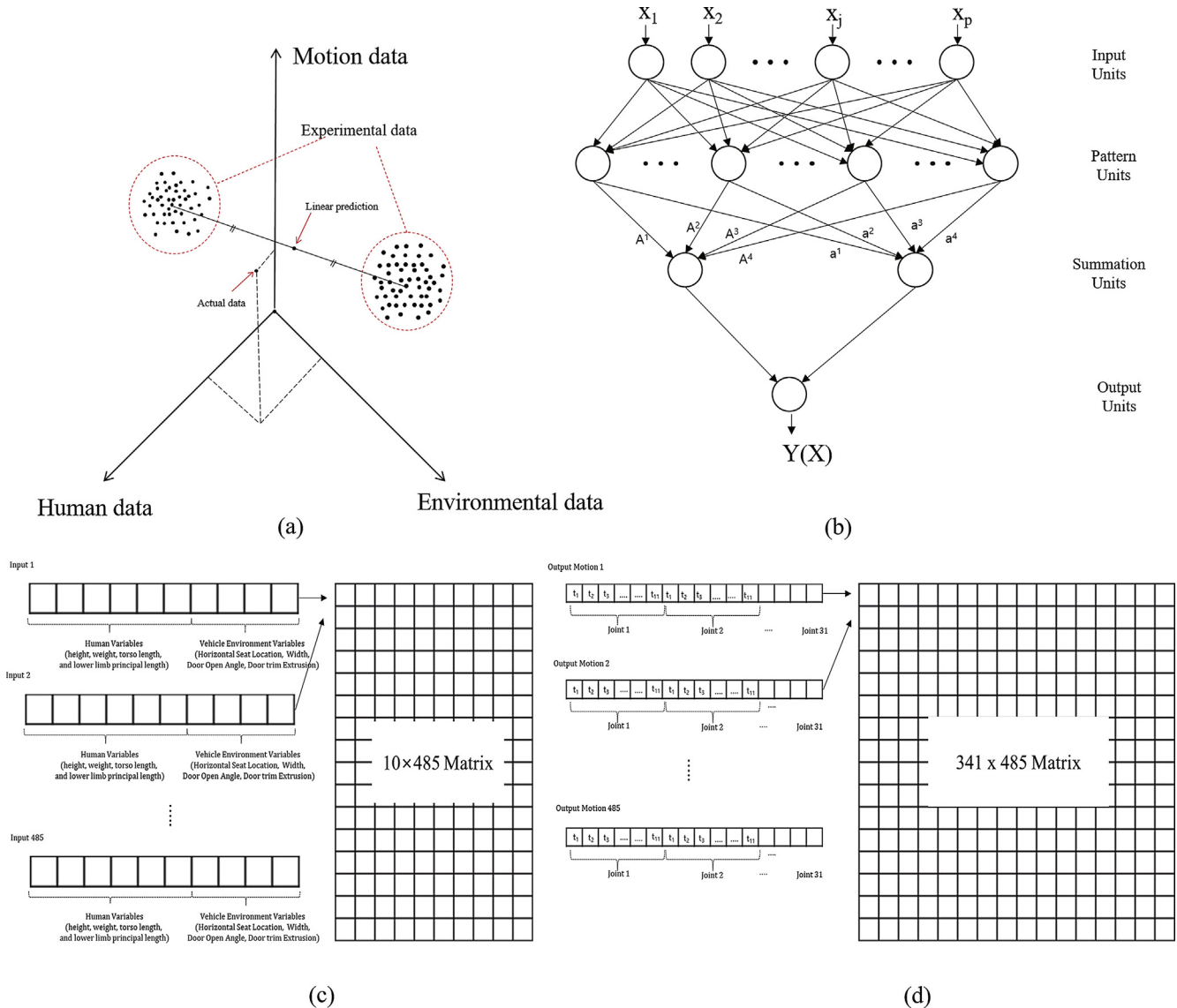


Fig. 2. Detail of the neural network. (a) Limitation of the linear prediction. (b) Block diagram of the network. (c) Input matrix information. (d) Output matrix information.

proposed method to generate a motion once the trained motion network is derived, surpassing the results of previous research (Bataineh et al., 2016). To verify the motion generated by the proposed algorithm, we constructed a test set composed of 15 pairs of actual motion and environment. All data in a test set did not participate the training procedures and were used only for statistical evaluation. This study compared 15 generated motion with 15 actual motion. For the interactive analysis, a visual comparison of resulting motion was performed. Fig. 3 shows snapshots of the experimental data and prediction data at four different times. As shown in the results, the motion task using the prediction data was realistic.

The first assessment process is a joint angle comparison. This research arbitrarily selects one motion and the corresponding environmental condition from the test sets and generates a motion from the environmental condition. As motion is generated, the generated results are compared with the experimental motion of the corresponding environment condition. The comparison between the lower body joint angles of the experimental and prediction data is shown in Fig. 4. Fig. 4 confirmed that the predicted kinematic profile is generally consistent with the actual experimental data. To quantify the comparison, the r-square value between actual joint curve and computed joint curve is calculated. The r-square of each joint is calculated in a domain with actual motion of each joint and predicted motion data of each joint set on the x-axis and y-axis, respectively. Table 1 shows the results

of a total of 31 DOF: pelvis – 6 DOF; right leg – 6 DOF; left leg – 6 DOF; lumbar – 3 DOF; right arm – 5 DOF; left leg – 5 DOF. This information allowed the study to compare relative accuracy of each joint. In the results, pronation of the left arm and shoulder adduction of the left arm show the low similarity. Except for these joints, the results confirmed a pattern of consistent similarity.

The second assessment was conducted by using the R-squared value of the control points. In this assessment, the entire 15 test sets are taken into account with 31 DOF for each set. Each DOF contained 11 control points. Therefore, a total of 5115 points (15 test set \times 31 DOF \times 11 control points) are utilized for the assessment to evaluate an overall accuracy of the prediction. As a result, an overall performance in motion prediction of the proposed algorithm was derived as Fig. 5. In Fig. 5, the control points obtained from the experiment and the control points obtained from the prediction are represented in the x-axis and y-axis, respectively. Fig. 5 demonstrates that the points converge in the centerline. The obtained statistical parameter values also show a high similarity. The calculated R-squared value was 0.9525, indicating a high level of similarity between experiment and prediction data. Furthermore, the calculated f-value is 1.025e+5 and calculated p-value is 0.0000. This p-value shows statistical significance of our results. Therefore, the predicted human motion in this study has a high level of accuracy.

The third assessment process was a trajectory comparison of the farthest distal segment COM. Because the digital human model

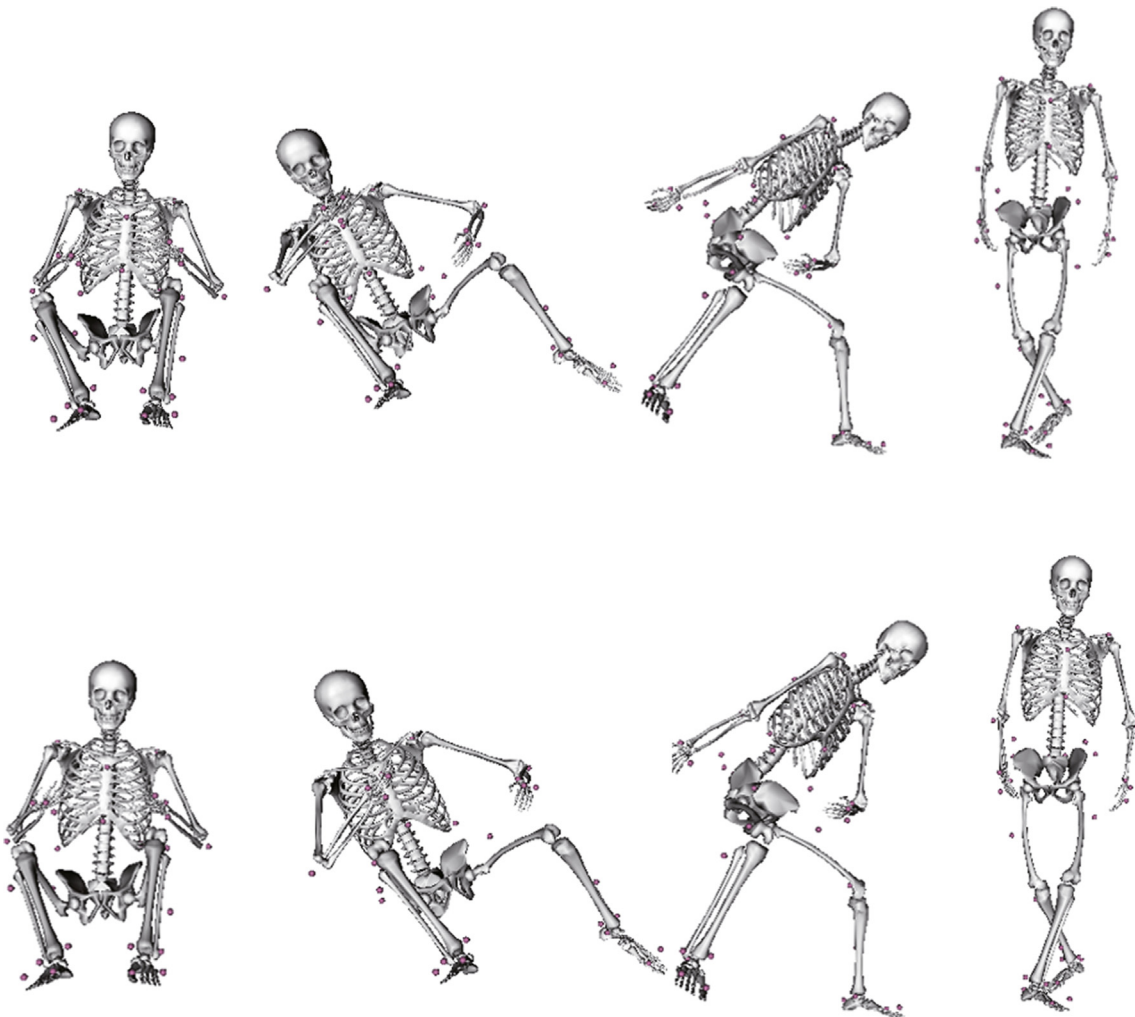


Fig. 3. Visual comparison of motion task. (a) Experiment data. (b) Prediction data.

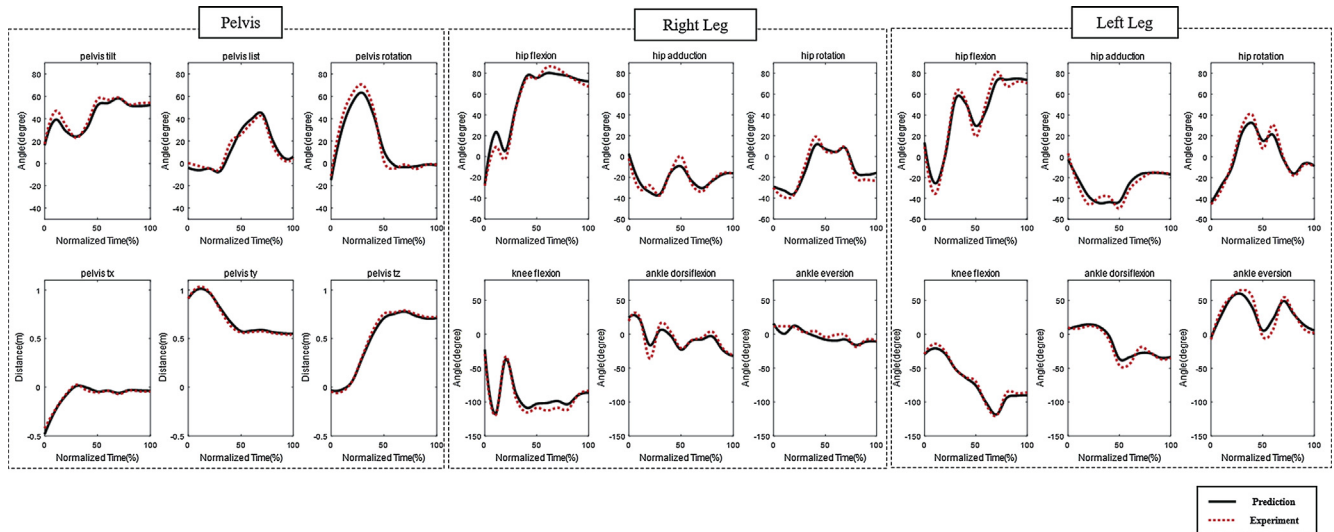


Fig. 4. Comparison of lower body joint angles.

Table 1
R-square results of joint comparison.

Segment	Joint Name	R-square
Pelvis	Pelvis tilt	0.9637
	Pelvis list	0.9670
	Pelvis rotation	0.9795
	Pelvis translation (X-direction)	0.9895
	Pelvis translation (Y-direction)	0.9962
	Pelvis translation (Z-direction)	0.9983
Right Leg	Hip flexion	0.9884
	Hip adduction	0.8266
	Hip rotation	0.9557
	Knee flexion	0.9708
	Ankle dorsiflexion	0.8647
	Ankle Eversion	0.7926
Left Leg	Hip flexion	0.9749
	Hip adduction	0.8836
	Hip rotation	0.9773
	Knee flexion	0.9917
	Ankle dorsiflexion	0.9529
	Ankle Eversion	0.9240
Lumbar	Lumbar extension	0.9805
	Lumbar bending	0.9214
	Lumbar rotation	0.9383
Right Arm	Shoulder flexion	0.9463
	Shoulder adduction	0.7119
	Shoulder rotation	0.9711
	Elbow flexion	0.9926
	Arm pronation	0.9065
Left Arm	Shoulder flexion	0.9079
	Shoulder adduction	0.5968
	Shoulder rotation	0.8414
	Elbow flexion	0.9765
	Arm pronation	0.5052

is represented by a tree structure, the difference in joint angle is propagated from the root segment to the farthest distal segment. Therefore, the overall prediction error can be analyzed in a conservative way by comparing the farthest distal segment. As shown in Fig. 6, this assessment graphically compares the three-dimensional trajectory of the left foot COM, the farthest distal segment, in the experimental and the predicted results. Fig. 6 shows that the trajectories of both the points are similar in three-dimensional space. Based on the results, we can confirm the similarity between the three-dimensionality of the motion generated by the proposed algorithm and the actual human motion.

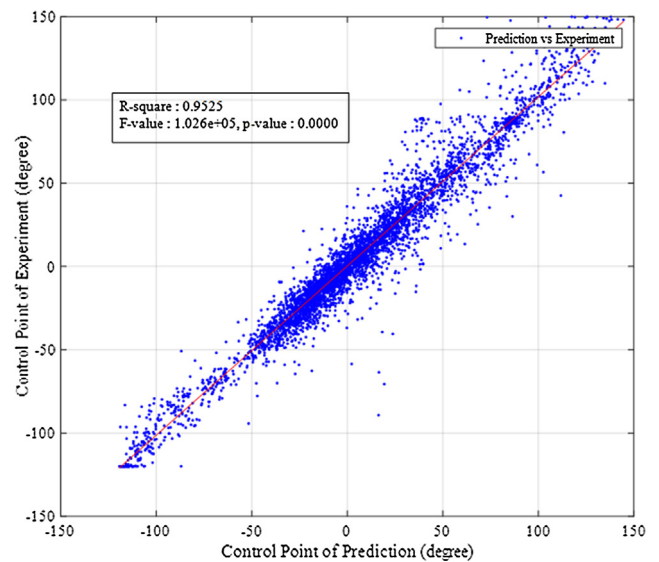


Fig. 5. Comparison graph of the control points.

4. Discussion

We developed a motion prediction algorithm for a full-body skeletal model with 31 DOF based on an ANN prediction algorithm. We validated the predicted results with the actual experimental results. The first assessment method compared the joint angles of the lower limbs and used statistical parameters to analyze them. The overall statistical parameters showed high similarity, but there was a difference in pronation (left arm). Experimental data for pronation showed big fluctuation in the 70% phase, but the prediction data showed smooth movement. This resulted fairly big difference between experimental data and prediction data. This phenomenon showed that the proposed algorithm might be limited in predicting the movement of certain joints. A similar pattern could be found in the result of the shoulder adduction joint. To find a reasonable explanation, our research team concentrated on the relationship between joint movement and prediction accuracy. Fig. 7 and Table 2 show the correlation between movement variation and similarity. We selected a joint with the lowest similarity in each segment and compared the r-square value with the maxi-

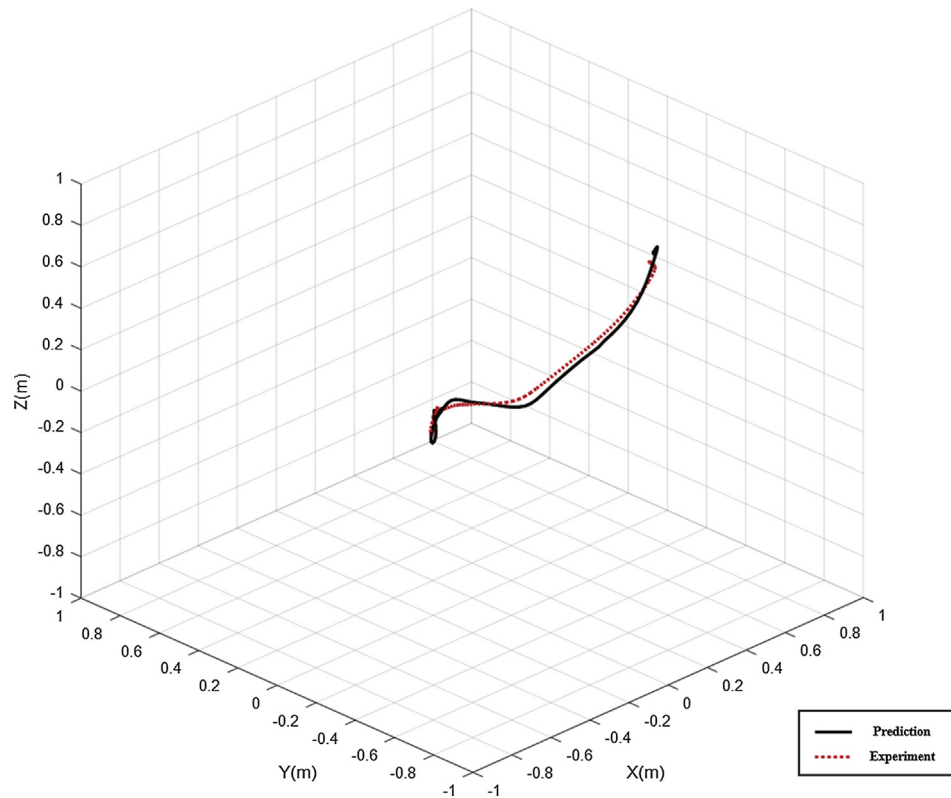


Fig. 6. Comparison graph of the foot center of mass trajectory.

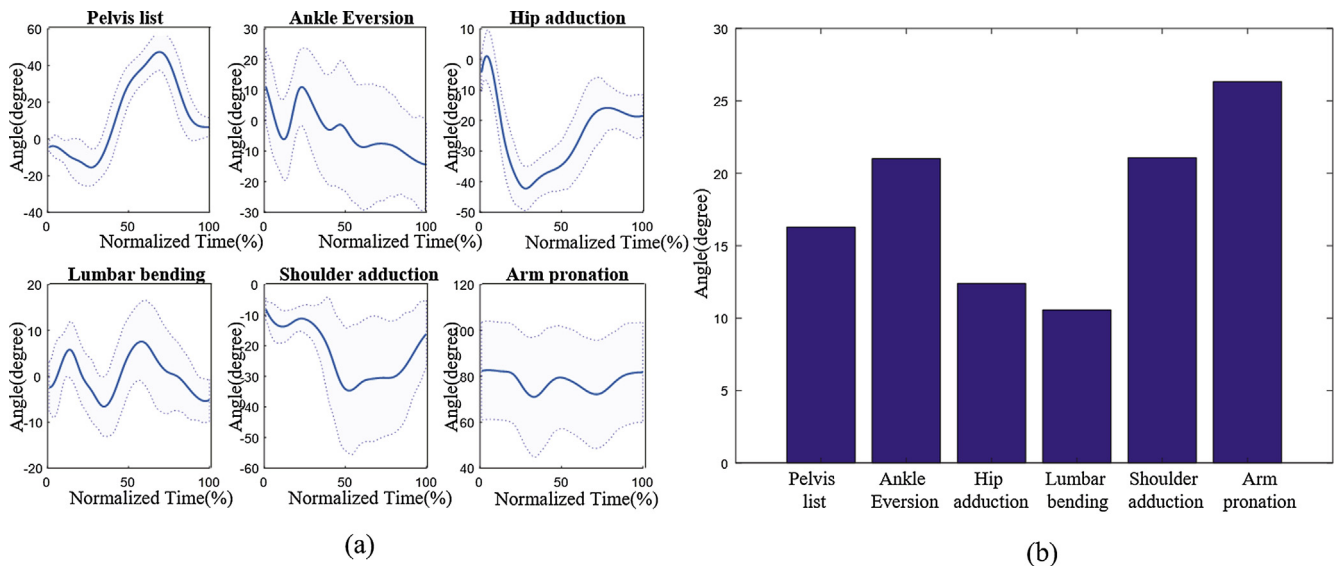


Fig. 7. (a) 1-sigma interval range graph of lowest joints. (b) Maximum standard deviation of lowest joints.

imum standard deviation of its motion. The similarity between experiment and simulation results is represented by the r-square value, and the movement variation of joints among individual subjects is represented by the maximum standard deviation. In Fig. 7 (a), the graphs represent 1-sigma interval ranges of the six lowest similarity joints. Fig. 7(b) shows the maximum standard deviation of each joint motion. As shown in Fig. 7(a) and (b), pronation of the left arm shows the greatest variation, and the shoulder adduction joint of the right arm and ankle eversion of the right leg have the next greatest variations. This trend in movement variation can be

observed in the similarity as well. As shown in Table 2, the pronation of the left arm shows the lowest r-square value, and the shoulder adduction of the right arm and the ankle eversion of the right leg have the next lowest r-square value. This correspondence between movement variation and similarity demonstrates that the proposed algorithm has lower prediction accuracy for joints with big movement variation among individual subjects. This is a limitation when predicting movement that has bigger variation using a small data set and insufficient input parameters to cover bigger variation among individuals. This study selected 6 human

Table 2

Segment and lowest similarity joint, R-square, maximum standard deviation information.

Segment	Lowest similarity joint	R-square	Maximum standard deviation (°)
Pelvis	Pelvis list	0.9670	16.28
Right leg	Ankle Eversion	0.7926	21.01
Left leg	Hip adduction	0.8836	12.39
Lumbar	Lumbar bending	0.9214	10.56
Right arm	Shoulder adduction	0.7119	21.09
Left arm	Arm pronation	0.5052	26.34

parameters to represent human anthropometric and movement characteristics. Although these parameters demonstrated high accuracy in overall movement and most joint movement, it demonstrated low accuracy in some joints that have big variation among individuals. However, increasing input parameters to achieve improved accuracy would require a larger data set. Because of the limited data set available, we chose small input parameters, which caused low accuracy for the joints with big movement variation among individuals. This issue could be solved by using a larger data set and more input parameters to accommodate variety in the individual subjects. The relationship between the size of dataset and prediction accuracy is shown in Appendix.

To evaluate the overall performance of proposed algorithm, we perform a second and a third assessment process. The second assessment compares the entire control points of the joint angle curves from prediction and experiment using the R-square value. As mentioned in the results, the R-square value was obtained to be 0.95251, which indicates a high level of similarity between experiment data and prediction data. The third assessment compares the trajectory of the center of the mass of the farthest segment. This assessment method provides another comparison criterion of overall performance because the difference in joint angle is propagated to the farthest distal segment. As Fig. 6 shows, trajectories of prediction and experiment are similar in three-dimensional space. Based on the second and third assessment results, we can confirm that our algorithm generates movement similar to actual human motion.

Theoretically, the proposed motion prediction algorithm is inspired by how real human beings create motion in various environmental conditions. Human behavior for a particular situation is generated from experiences in which a similar motion was previously performed. In this study, we attempted to implement this process through a motion capture database and an ANN. Captured human motion in a variety of environments was used to construct a motion database that functioned as “past motion experience” when a new environment was encountered. In the “recall of past experience” process, an ANN was used. ANNs, inspired by the human cognitive system, generate highly accurate motion in new environments, as shown above. They overcome the high complexity and nonlinearity of human motion, which are limitations of linear prediction. Furthermore, the proposed algorithm overcomes the limitations of previous motion capture-based approaches and provides human motion that continuously responds to various environmental changes. Moreover, it not only guarantees faster results than existing research methods based on optimization but also makes it possible to avoid the ambiguity of the objective function of human motion. In addition, our work is based on actual human motion, which enhances the reliability of the generated motion. In this research, we proved the ability of ANNs to predict actual human motion that is acyclic and complex. The proposed algorithm could be useful when studying simulations of the if-then scenarios that have not actually been experimentally investigated yet. Furthermore, this research could be adapted in various human-product

integrated design and biomechanical fields due to its ability to transform a discontinuous database into a continuous motion profile. In particular, the proposed algorithm, which guarantees high speed and accuracy, can be applied to various industrial fields. One thing to discuss further is that the proposed algorithm yielded low accuracy for joints with big variation. Although the proposed algorithm shows high accuracy in overall movement and most joint movement, it showed low prediction accuracy in some joints that have big variation among individuals. Therefore, the proposed algorithm has limitations in predicting the movement of joints with big variation among individual subjects. This phenomenon might be due to the relatively small number of input parameters and data set, and it could be improved through the use of a more detailed input parameters and larger motion data set that reflects the variety in individual subjects. Also, the proposed algorithm used normalized control point for training, so it could not include temporal information. Considering temporal information in training the motion experience and predicting motion in large environment variations would yield more useful results.

Acknowledgements

The Institute of Engineering Research at Seoul National University provided research facilities for this work.

Conflict of interest

As far as the authors know there is no conflict of interest in this manuscript. This paper has been neither published nor submitted elsewhere for publication, in whole or in part, either in a serial, professional journal or as a part in a book that is formally published and made available to the public.

Appendix A. Supplementary material

Supplementary data to this article can be found online at <https://doi.org/10.1016/j.jbiomech.2018.12.009>.

References

- Abdel-Malek, K., Arora, J., 2013. *Human Motion Simulation: Predictive Dynamics*. Academic Press.
- Aggarwal, J.K., Cai, Q., 1999. Human motion analysis: A review. *Comput Vis Image Underst.* 73, 428–440.
- Bataineh, M., Marler, T., Abdel-Malek, K., 2013. Artificial neural network-based prediction of human posture. In: *International Conference on Digital Human Modeling and Applications in Health, Safety, Ergonomics and Risk Management*.
- Bataineh, M., Marler, T., Abdel-Malek, K., Arora, J., 2016. Neural network for dynamic human motion prediction. *Exp. Syst. Appl.* 48, 26–34.
- Bataineh, M.H., 2015. *New neural network for real-time human dynamic motion prediction*. The University of Iowa.
- Bu, N., Okamoto, M., Tsuji, T., 2009. A hybrid motion classification approach for EMG-based human-robot interfaces using bayesian and neural networks. *IEEE Trans. Rob.* 25, 502–511.
- Chaffin, D.B., 2002. On simulating human reach motions for ergonomics analyses. *Hum. Fact. Ergon. Manuf. Serv. Ind.* 12, 235–247.
- Davis III, R.B., Ounpuu, S., Tyburski, D., Gage, J.R., 1991. A gait analysis data collection and reduction technique. *Hum. Mov. Sci.* 10, 575–587.
- Delp, S.L., Anderson, F.C., Arnold, A.S., Loan, P., Habib, A., John, C.T., Guendelman, E., Thelen, D.G., 2007. OpenSim: open-source software to create and analyze dynamic simulations of movement. *IEEE Trans. Biomed. Eng.* 54, 1940–1950.
- Dretsch, M.N., Tipples, J., 2008. Working memory involved in predicting future outcomes based on past experiences. *Brain Cogn.* 66, 83–90.
- Farahani, S.D., Svinin, M., Andersen, M.S., de Zee, M., Rasmussen, J., 2016. Prediction of closed-chain human arm dynamics in a crank-rotation task. *J. Biomech.* 49, 2684–2693.
- Fernando, T., Maier, H., Dandy, G., 2009. Selection of input variables for data driven models: an average shifted histogram partial mutual information estimator approach. *J. Hydrol.* 367, 165–176.
- Fregly, B.J., 2009. Design of optimal treatments for neuromusculoskeletal disorders using patient-specific multibody dynamic models. *Int. J. Comput. Vision Biomech.* 2, 145.

- Gerus, P., Sartori, M., Besier, T.F., Fregly, B.J., Delp, S.L., Banks, S.A., Pandy, M.G., D'Lima, D.D., Lloyd, D.G., 2013. Subject-specific knee joint geometry improves predictions of medial tibiofemoral contact forces. *J. Biomech.* 46, 2778–2786.
- Hamner, S.R., Seth, A., Delp, S.L., 2010. Muscle contributions to propulsion and support during running. *J. Biomech.* 43, 2709–2716.
- Jung, M., Cho, H., Roh, T., Lee, K., 2009. Integrated framework for vehicle interior design using digital human model. *J. Comput. Sci. Technol.* 24, 1149–1161.
- Kim, S., Lee, K., 2009. Development of discomfort evaluation method for car ingress motion. *Int. J. Automot. Technol.* 10, 619–627.
- Kim, T., Lee, K., Kwon, J., 2012. Design improvement of the smith machine using simulation on musculoskeletal model. *Int. J. CAD/CAM* 12.
- Kumar, D., Swanik, C.B., Reisman, D.S., Rudolph, K.S., 2014. Individuals with medial knee osteoarthritis show neuromuscular adaptation when perturbed during walking despite functional and structural impairments. *J. Appl. Physiol.* 116, 13–23.
- Lee, L.-F., Narayanan, M.S., Kannan, S., Mendel, F., Krovi, V.N., 2009. Case studies of musculoskeletal-simulation-based rehabilitation program evaluation. *IEEE Trans. Rob.* 25, 634–638.
- Marra, M.A., Vanheule, V., Fluit, R., Koopman, B.H., Rasmussen, J., Verdonschot, N., Andersen, M.S., 2015. A subject-specific musculoskeletal modeling framework to predict in vivo mechanics of total knee arthroplasty. *J. Biomech. Eng.* 137, 020904.
- Masoud, H.I., Reed, M.P., Paynabar, K., Wang, N., Jin, J.J., Wan, J., Kozak, K.K., Gomez-Levi, G., 2016. Predicting subjective responses from human motion: application to vehicle ingress assessment. *J. Manuf. Sci. Eng.* 138, 061001.
- Masoud, H.I., Zerehsaz, Y., Jin, J.J., 2017. Analysis of human motion variation patterns using UMPCA. *Appl. Ergon.* 59, 401–409.
- Moeslund, T.B., Hilton, A., Krüger, V., 2006. A survey of advances in vision-based human motion capture and analysis. *Comput. Vis. Image Underst.* 104, 90–126.
- Oh, S.E., Choi, A., Mun, J.H., 2013. Prediction of ground reaction forces during gait based on kinematics and a neural network model. *J. Biomech.* 46, 2372–2380.
- Rasmussen, J., Dahlquist, J., Damsgaard, M., de Zee, M., Christensen, S.T., 2003. Year Musculoskeletal modeling as an ergonomic design method. In: International Ergonomics Association XVth Triennial Conference.
- Rasmussen, J., Dahlquist, J., Damsgaard, M., de Zee, M., Christensen, S.T., 2000. Musculoskeletal modeling as an ergonomic design method. In: International Ergonomics Association XVth Triennial Conference.
- Specht, D.F., 1991. A general regression neural network. *IEEE Trans. Neural Networks* 2, 568–576.
- Wagner, M.J., Smith, M.A., 2008. Shared internal models for feedforward and feedback control. *J. Neurosci.* 28, 10663–10673.
- Xiang, Y., Arora, J.S., Rahmatalla, S., Abdel-Malek, K., 2009. Optimization-based dynamic human walking prediction: one step formulation. *Int. J. Numer. Meth. Eng.* 79, 667–695.
- Zhang, B., Horváth, I., Molenbroek, J.F., Snijders, C., 2010. Using artificial neural networks for human body posture prediction. *Int. J. Ind. Ergon.* 40, 414–424.